LA-6761

C.3

UC-34c

Issued: June 1977

Neutron Total Cross-Section Measurements of ^{9}Be, $^{10,11}B$, and $^{12,13}C$ from 1.0 to 14 MeV Using the $^{9}Be(d,n)^{10}B$ Reaction as a "White" Neutron Source

G. F. Auchampaugh
C. E. Ragan, III
S. Plattard*
N. W. Hill**

*Consultant. Centre d' Etudes de Bruyères-le-châtel, BP561, 92542 Montrouge Cedex, France.
**Visiting Scientist. Oak Ridge National Laboratory, Oak Ridge, TN 37830.

los alamos
scientific laboratory
of the University of California
LOS ALAMOS, NEW MEXICO 87545

An Affirmative Action/Equal Opportunity Employer

UNITED STATES
ENERGY RESEARCH AND DEVELOPMENT ADMINISTRATION
CONTRACT W-7405-ENG. 36

Printed in the United States of America. Available from
National Technical Information Service
U.S. Department of Commerce
5285 Port Royal Road
Springfield, VA 22161
Price: Printed Copy $3.50 Microfiche $3.00

NEUTRON TOTAL CROSS-SECTION MEASUREMENTS OF ^{9}Be, ^{10,11}B, AND ^{12,13}C FROM 1.0 TO 14 MeV USING THE ^{9}Be(d,n)^{10}B REACTION AS A "WHITE" NEUTRON SOURCE

by

G. F. Auchampaugh, C. E. Ragan, III,
S. Plattard, and N. W. Hill

ABSTRACT

High-resolution and high-accuracy total cross sections of ^{9}Be, ^{10,11}B, and ^{12,13}C have been measured from 1.0 to 14 MeV. The Los Alamos Scientific Laboratory (LASL) tandem accelerator was used to produce a "white" source of neutrons by stopping a pulsed beam of 15-MeV deuterons in a thick beryllium target. The neutron energy resolution [full width at half maximum (FWHM)] achieved in kiloelectron volts is given by $1.4E(MeV)^{3/2}$, and the accuracy of the neutron energy scale in kiloelectron volts is given by $\pm 0.060E(MeV)\sqrt{1.79E(MeV) + 0.75}$. The statistical uncertainties in the transmission vary from 0.5% to 2%, and the systematic error in the transmission is estimated to ±1.7%. The high statistical accuracy of the ^{11}B data, for example, has revealed fine structure at high excitation energy (around 9 MeV) which correlates with the structure observed in charged-particle measurements on the same compound nucleus. There are also indications of additional structures that have not been seen previously in the ^{12}B compound nucleus at this excitation energy.

I. INTRODUCTION

This program was begun to provide a set of high-quality cross sections on the light isotopes for nuclear structure studies. The paucity of data in the million-electron-volt region on some of these isotopes in the ENDF cross-section library, for example, is surprising in view of their importance to the US energy program. There were essentially no total cross-section data available in the million-electron-volt region on the isotopes ^{10,11}B, and yet the total cross section, in principle, is one of the easiest cross sections to measure with high accuracy. If available, they could be used to infer some of the partial cross sections that are more difficult to measure.

We therefore decided to measure the total cross sections of ^{9}Be, ^{10,11}B, and ^{12,13}C with high statistical as well as absolute accuracy and with good resolution. These data would not only serve as a basis for nuclear structure studies but would have the necessary quality to fill some of the gaps in the ENDF library. The ^{9}Be and ^{12}C nuclei were included to check the experimental technique since high-quality, total cross-section data already exist on these isotopes in the ENDF library. The ^{13}C + n nucleus is interesting for theoretical considerations because the A = 14 system should be amenable at

low excitation energy to shell-model calculations that for simple configurations would consist of two neutrons coupled to a ^{12}C core.

For several decades Van de Graaff accelerators have played a major role in the study of neutron-induced reactions in the million-electron-volt energy region by providing beams of monoenergetic neutrons using the reactions $^{7}Li(p,n)$, $^{3}H(d,n)$, $^{3}H(p,n)$, and $^{2}H(d,n)$. The high neutron energy resolution that can be achieved with these reactions and the monochrometicity of the neutron beam have made the Van de Graaff a powerful and useful tool in neutron physics.

Recently, the Van de Graaff has been used to produce a continuous or "white" source of million-electron-volt neutrons for neutron physics research using the $^{9}Be(d,n)$ reaction.[1] In such a system the deuterons are bunched into pulses of less than 1-ns width at repetition rates up to several megacycles and stopped in a beryllium target. Using subnanosecond time-of-flight (TOF) techniques with a 40-m flight path, for example, the energy resolution that can be achieved is comparable to that realized with monochromatic neutron sources.

In Sec. II we shall compare the characteristics of the beryllium neutron source to the more conventional "white" neutron sources using linear accelerators (LINACs). In addition, we shall discuss how the beryllium source was used in these measurements. In Sec. III we shall discuss the data reduction and in Sec. IV the results.

II. EXPERIMENTAL DETAILS

A. Van de Graaff

The Los Alamos Scientific Laboratory (LASL) tandem accelerator was used to accelerate deuterons to an energy of 15 MeV. An Ortec* duoplasmatron source equipped with a klystron buncher provided deuterons in a pulsed beam with a width of less than 1 ns and with a fundamental frequency of 5 MHz. To prevent overlap of the lowest energy neutrons detected (0.8 MeV) in the measurement with the high-energy neutrons from the next pulse, this frequency was reduced to 312 kHz by selecting every 32nd deuteron pulse. The average current on target obtainable at this frequency is about 400 nA although the currents actually used in the measurements were somewhat less. The target was cooled by compressed air.

*100 Midland Rd., Oak Ridge, TN 37830.

B. Beryllium "White" Neutron Source

1. Neutron Energy Distribution. The neutron yield (n/keV·s·sr) measured at 0° with respect to the deuteron beam for 15-MeV deuterons incident on a beryllium target is given by the solid line in Fig. 1. The data are for a 1-ns-wide deuteron pulse and a current of 400 nA. The Q-value for the $^{9}Be(d,n)^{10}B$ reaction is 4.3607 MeV (Ref. 2), which means that the distribution has a maximum neutron energy of 19.24 MeV. The pronounced discontinuities in the distribution, particularly at about 13.9 MeV, correspond to excited states in the residual nucleus ^{10}B.

The neutron yield from the beryllium reaction for 1-ns equivalent neutron resolution is compared in

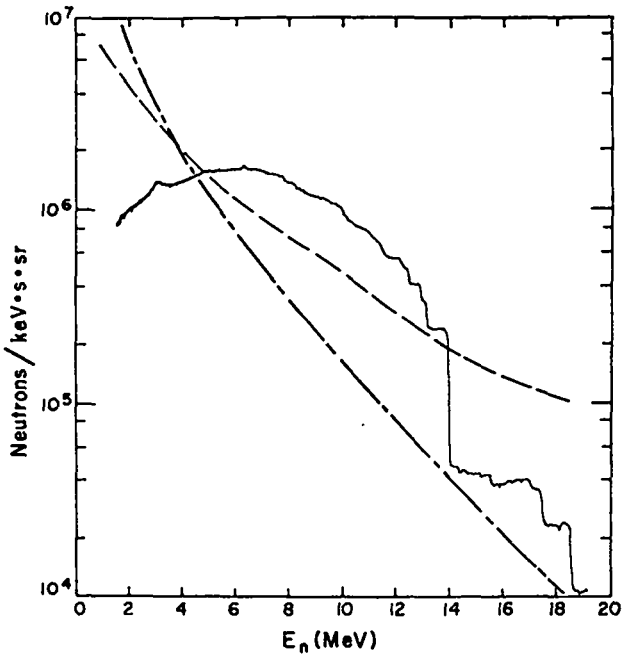

Fig. 1.
The observed neutron yields from the $^{9}Be(d,n)^{10}B$ reaction at LASL (——), the calculated yields from the bare tungsten target at LAMPF (— —), and the observed yields from the bare tantalum target at ORELA (— - —) for a 1-ns equivalent neutron timing resolution.

Fig. 1 with that from the Oak Ridge Electron Linear Accelerator (ORELA) and from a new pulsed neutron facility at the Los Alamos Meson Physics Facility (LAMPF). The ORELA data are for a bare tantalum target measured at 90° to the direction of the electron beam for a 5-ns-wide pulse and for an electron beam power of 12 kW. The data have been divided by the square of the ratio of electron-pulse width to the deuteron-pulse width to compare with the 1-ns beryllium data. Above about 1 MeV the neutron energy resolution of the target is essentially determined by the width of the electron pulse; therefore, the flight path would have to be increased by this ratio and consequently the yield would have to be reduced by the square of this ratio. The LAMPF data represent the 90° yield calculated for a 2.54-cm-diam by 15-cm-long tungsten target bombarded 120 times/s by 800-MeV protons with an average beam current of 10 nA. A 1-ns neutron-pulse width was used to put the LAMPF data on a common resolution basis even though the actual pulse width will increase from about 500 ps at 10 MeV to 2 ns at 1 MeV for this target geometry. The parameters chosen for this comparison represent reasonable operating conditions for the various neutron sources.

This comparison shows that a Van de Graaff accelerator, when used as a source of "white" neutrons, is competitive with current LINAC neutron sources over a wide energy range. It also shows the potential capabilities of a pulsed Van de Graaff facility as a "white" source of million-electron-volt neutrons, which could be achieved if the full dc deuteron beam (approximately 60 μA for our duoplasmatron) could be bunched into 1-ns pulses at a useful repetition rate. The capability for achieving this is well within current accelerator technology.

2. Neutron Pulse Width. The width of the neutron pulse from the target is limited primarily by the width of the deuteron pulse; the slowing down of the deuteron in the target contributes less than 50 ps to the width. The readily achievable and stable deuteron-pulse width from the LASL tandem accelerator is about 1 ns although we have observed a stable deuteron-pulse width of less than 0.8 ns when the buncher was properly tuned. The shape of the deuteron pulse can be well represented by a Gaussian function.

3. Other Desirable Characteristics. The intensity of the "gamma flash," caused by gamma-ray decay of the excited states formed in the beryllium reaction, is sufficient to permit its use as a time fiducial. However, it is not intense enough to overload the detector electronics, and therefore measurements can be made up to the maximum neutron energy produced in the reaction.

The small volume of the neutron source (~ 5 mm^3) has several obvious advantages: First, it provides a point source geometry that simplifies the design of a neutron collimation system. Second, the close collimation obtained is amenable to small samples, which is a significant advantage in measurements with separated isotopes.

The neutron and gamma-ray background from neutron capture reactions is much less with the beryllium source than with conventional sources because only neutrons in the energy region of interest to the measurement are produced in the target.

The low instantaneous neutron production rate yet high average rate from the target means that highly statistically significant data can be acquired in a relatively short time (hours) with very low deadtime losses (few per cent) for experiments that use the neutron beam directly, such as a total cross-section measurement. In contrast, the relatively low repetition rate yet high intensity available with LINAC-based sources generally results in large deadtime losses.

C. Layout

A schematic drawing of the LASL TOF facility is shown in Fig. 2. A quadrupole lens focuses the deuteron beam to a 2.5-mm-diam spot onto a 1-mm-thick beryllium target that is approximately 3 m from the lens. A 5-mm-diam gold collimator located upstream of the target ensures proper alignment of the deuteron beam with respect to the axis of the neutron collimation system. The collimator current is adjusted to zero to eliminate neutron background from the collimator. The range of 15-MeV deuterons in beryllium is about 0.8 mm.

The neutron collimation system consists of a 61.9-cm-long by 15-cm-diam primary brass collimator, which has a 0.696-cm-diam hole along the cylindrical axis, and two brass scraper collimators

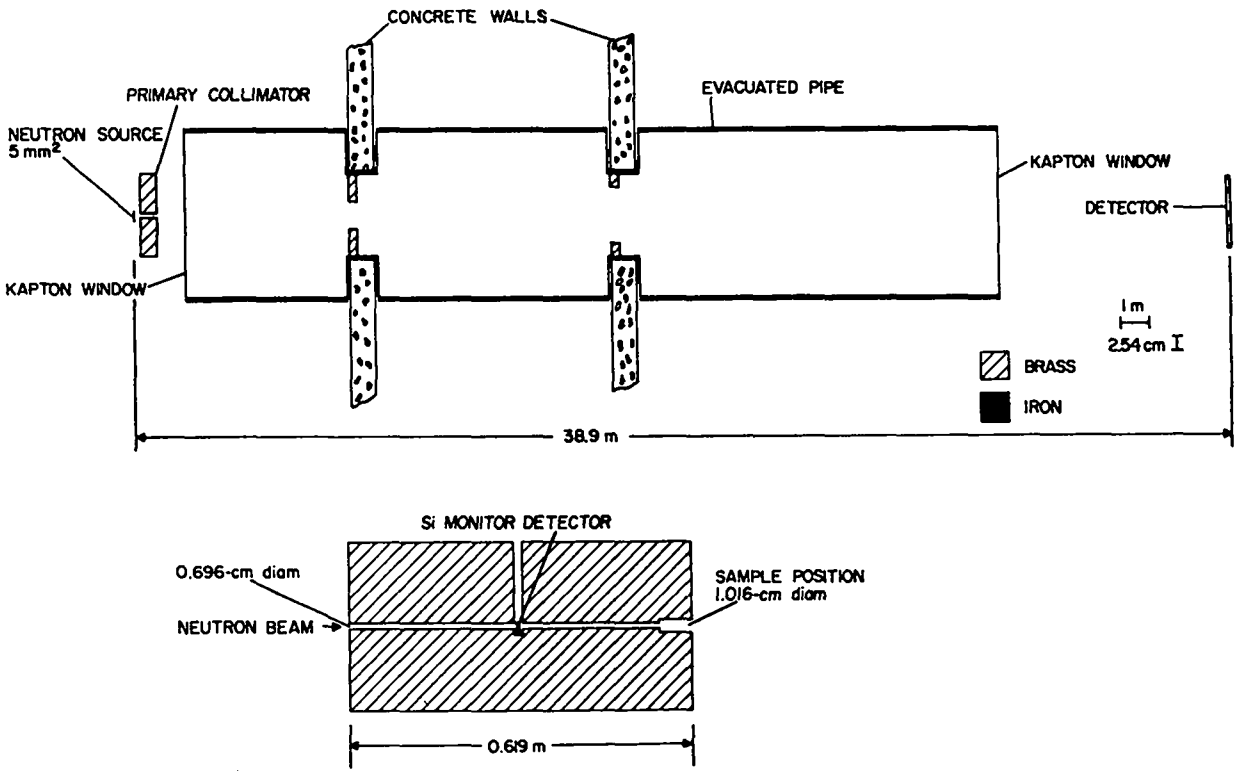

Fig. 2.
The 40-m flight path at the LASL tandem accelerator used for neutron total cross-section measurements.

each 30 cm long. The primary collimator is about 15 cm from the target and the scraper collimators are in concrete walls, one of which forms the wall of the room containing the neutron source and the other forms the outside wall of the room adjacent to the neutron source room. The diameter of the neutron beam at the detector position is about 20 cm. The scraper collimators restrict the field of view of the detector to a diameter of less than the outside diameter of the primary collimator, which prevents the detector from seeing the walls of the neutron room.

The neutron detector was located at a nominal distance of 38.92 m from the beryllium target in a thin-walled, temperature-controlled portable building. The detector was supported by a low-mass table and was not surrounded by any shielding material. The vacuum windows consisted of 125-μm-thick Kapton* ($C_{16}H_8O_4N_2$, ρ = 1.42 g/cm^3).

*DuPont, 1007 Market St., Wilmington, DE 19898.

The sample changer was fastened to the detector end of the primary collimator. Upon receiving a command from the data acquisition computer, it would automatically insert one of two samples into the 1.016-cm-diam hole at the end of the collimator.

D. Neutron Detectors

A NE-110 plastic scintillator* was used in the beryllium and carbon measurements as a neutron detector. It had a diameter of 12.7 cm and a center thickness of 2.2 cm. The plastic was machined to fit directly onto the photocathode surface of an RCA 8854 photomultiplier tube.** The anode signal was shaped by an Ortec 463 constant fraction discriminator (CFD) that provided the fast "start" pulse for an EG&G TDC 100 time digitizer.† The

*Nuclear Enterprise, 935 Terminal Way, San Carlos, CA 94070.
**RCA Corp., 4546 El Camino Real, Los Altos, CA 94022.
†EG&G, Inc., Oak Ridge, TN 37830.

dynode signal was sent to a differential discriminator that was set for a neutron energy window of 0.8-20 MeV and provided a coincidence pulse for the start signal. The "stop" pulse came from a pick-off coil preceding the gold collimator through which the deuteron beam passed. Typical open-beam (sample-out) counting rates at 400 nA were 20 000 counts/s.

The overall time response of the NE-110 detector was determined by using the narrow resonances in $^{16}O + n$ at 3.210 MeV and in $^{18}O + n$ at 2.650 MeV. The natural width of the ^{16}O resonance at our flight path is less than 0.3 ns. The ^{18}O resonance has not been previously observed. Both resonances had an observed width of 1.8 ± 0.1 ns. The FWHM of the gamma-ray peak was 1.63 ± 0.5 ns. The difference between the two times can be attributed to the finite flight time of the neutron in the scintillator before it creates a light pulse.

A Pilot-U scintillator* was used for the boron measurements. It had a diameter of 10 cm and a center thickness of 1.25 cm. Instead of using a fast-slow system for the timing signal as was used for the other measurements, a fast-fast system was set up. It consisted of a fast Le Croy amplifier (LRS 612),** to provide two identical anode signals, and two Canberra 1428 CFDs.† One CFD was set at a very low threshold for the fast timing pulse and the other was set at a threshold corresponding to a neutron energy of 0.8 MeV. Rather than use the coincidence circuit provided in the start circuit of the digitizer, we used an external coincidence unit (LRS 365 AL)** for both the timing and energy signals.

This detector was designed to have good timing for a large dynamic range to take advantage of the 1-ns capabilities of the buncher system. Using a ^{60}Co source we measured a time resolution of 750 ± 50 ps for a dynamic range of 200:1. Unfortunately the buncher could not be adjusted to give a deuteron-pulse width narrower than about 1.8 ns during these measurements. The measured FWHM of the gamma-ray peak was 2.0 ± 0.1 ns. Therefore the resolution of the boron data is somewhat poorer than that of the beryllium and carbon data.

*Nuclear Enterprise.
**Le Croy Research Systems Corp., 700 S. Main St., Spring Valley, NY 10977.
†Canberra Industries, 45 Gracey Ave., Meriden, CT 06450.

E. Monitor Detectors

1. Deuteron-Beam Width Detector. The width of the deuteron pulse was measured continuously during a measurement with a fast, plastic scintillator detector. It was positioned about 1 m from the beryllium target and consisted of a 1.9-cm-diam by 0.64-cm-thick piece of NE-110 plastic mounted on an RCA 8575 photomultiplier tube. The photomultiplier was connected to an Ortec-271 constant fraction timing base. The timing pulse from the base, which started a time-to-amplitude converter, was gated by a pulse from a differential discriminator fed by the dynode signal from the base. The discriminator window was set to make the intrinsic timing resolution of the detector much less than the width of the deuteron pulse. This width varied between 0.9 and 1.2 ns for the beryllium and carbon measurements and, as mentioned before, was as high as 1.8 ns in the boron measurements.

2. Neutron Beam Monitor. The relative neutron flux incident upon the sample was measured with a transmission-mounted silicon diode 150 mm^2 in diameter by 150 μm thick. The diode was inserted into the neutron beam inside the primary collimator 30 cm in front of the sample. The (n,p) and (n,α) reactions in the silicon provided a monitor of the neutron beam. A pulse-height spectrum was taken before and after each run to check the stability of the detector system. A bias was set at the minimum in the pulse-height distribution. All events greater than this bias were recorded and used to normalize the sample-in to sample-out runs. The degradation in pulse height due to radiation damage from high-energy neutrons was negligible even after the detector had been exposed to an integrated dosage of approximately 10^{18} n.

3. Deuteron Beam Monitor. The deuteron current was monitored during each run. If it varied by more than ±10% data acquisition stopped until the beam current was brought back to its previous value. The accumulated charge was recorded and used to control the sample-in to sample-out cycle time. The agreement between the neutron monitor (diode) results and the charge monitor for the

sample-in to sample-out time was better than 0.3% for a typical run.

F. Samples

The characteristics of the samples used in obtaining the final cross sections are given in Table I. The thicknesses are computed by accounting for the isotopic enrichment of the material and assuming that the material is chemically pure.

Each carbon and boron sample was fabricated from powder that was pressed into a cylinder with an inside radius of 0.381 cm and an outside radius of 0.501 cm. The ends were sealed with 0.15-cm-thick disks. For the boron measurements the cylinder material was brass and for the carbon measurements it was copper. The amount of water absorbed during the pressing operation was negligible because the narrow ^{16}O resonance at 1.651 MeV could not be seen in the data. A natural boron sample, which had 3.8 at.% water content, clearly showed this resonance. Empty cans fabricated from either copper or brass were used for the sample-out measurements. The beryllium sample was machined from metal into a rod that could be inserted into a blank copper cylinder.

G. Running Conditions

For the measurements on beryllium and carbon, the machine current was about 160 nA, and each run lasted for about 13 h. For the boron measurements the current was higher, about 360 nA, and each run was about one-half as long, or about 6 h. The sample-in to sample-out cycle time was kept at 3:1 with a complete cycle time of about 15 min.

H. Data Acquisition Program

To accommodate the high average data rates (5 000-18 000 counts/s) in these measurements and yet keep the computer deadtime minimal, a data acquisition program was written to use the memory increment mode of our XDS 930 computer. The average time to store an event was about 8 μs. The data were stored in 8192 memory words, each word representing a 0.5-ns channel. The program would read into memory from disc storage at the beginning of each cycle either the sample-in or sample-out spectrum, accumulate new data, and switch spectra at the end of the cycle. The program controlled the position of the sample and, upon request, would convert the raw data into cross sections. We could then use this information to determine whether the data were statistically adequate.

III. DATA REDUCTION

A. General

The reduction of transmission to cross section is straightforward once the data have been corrected for background and deadtime. These corrections will be discussed in detail in Secs. III.B and III.C. The

TABLE I

SAMPLE CHARACTERISTICS

Isotopic Enrichment (%)	Thickness (at/b)	Chemical Purity (%)	Major Impurity (%)
^{9}Be 100.0	0.3713 ± 0.0006	99.4	O < 0.9
^{10}B 96.19	0.4509 ± 0.0030	98.8	Si < 0.2; Zn < 0.2
^{11}B 97.15	0.4119 ± 0.0027	98.2	C < 1.23
^{12}C 99.95	0.3883 ± 0.0026	99.9	H_2O < 0.1
^{13}C 89.9	0.3584 ± 0.0024	99.9	H_2O < 0.1

neutron beam monitor was used to normalize the sample-in data to the sample-out data. The neutron energy corresponding to each 0.5-ns channel was computed relativistically using 939.5731 MeV for the neutron mass and knowing the relative time of the leading edge of a channel to that of the gamma-ray channel. The gamma-ray channel (zero-time fiducial) was corrected for the flight time of the gamma ray. The transmission was converted to an effective cross section. This cross section is somewhat different from the true cross section because of resolution effects that are distorted by the nonlinear relationship between cross section and transmission; i.e., the resolution in the cross section is much worse, especially for narrow resonances, than in the transmission, except for very small values of n. For this reason, n was kept as small as practicable and the channel width was chosen to be about one-quarter of the resolution width. Under these conditions the effective cross section approaches the true cross section, except for very narrow resonances.

B. Deadtime Correction

The data were corrected for those events that were lost because the time digitizer accepted only one event per beam pulse and because the buffer in the digitizer could be reset by the next event before the computer could accept the first event. This resulted in a very small correction to each channel (less than 0.2%). Since the time between beam pulses was 3.2 μs and the deadtime of the digitizer was 4 μs, there was no advantage to running the digitizer in the multiple stop-per-start mode. This simplified the procedure for correcting the data for multiple events per beam pulse.

The multiple event correction, for channel i in measured quantities, is given by the analytical function,

$$T_i = \frac{R_i}{1 - \frac{R_i}{2S} - \frac{1}{S} \sum_{c=i+1}^{M} R_c}$$

where T_i is the number of true counts in channel i, R_c is the number of recorded counts in channel c, S is the total number of start pulses for which there is a corresponding stop pulse, and ΣR_c is a sum from channel i + 1 to the maximum number of channels, M. This expression is valid as long as $(\Sigma R_c)/S$ is much less than 1 and as long as the neutron intensity remains constant.

For our measurements, $(\Sigma R_c)/S$ varied from 0 for the highest energy channel to about 0.03 for the lowest energy channel. As previously mentioned, the deuteron-beam current was monitored during a run, and if it varied by more than a preset amount, data acquisition was inhibited. Since the multiple pulse correction was less than a few per cent, a drift of $\pm$10% was considered an acceptable variation in beam intensity.

The procedure for correcting the data for deadtime losses was checked for a random spectrum with a gamma-ray source. The multiple-pulse deadtime and computer deadtime were varied both simultaneously and independently for deadtime losses of between 0% and 10%. The good agreement in the resulting spectra gave us confidence in our procedure for correcting data for lost events.

C. Background Corrections

The background spectrum usually consists of two parts, one that is independent of time and unrelated to the accelerator operation and one that depends upon time and is directly correlated with the neutron burst. The part of the time-independent background that is not associated with the accelerator but is due to the natural radioactivity in the vicinity of the detector and to cosmic rays can be measured by simply turning off the accelerator. However, the time-dependent background that arises from collimator scattering, leakage through walls, and room return from neutrons that scatter off the detector is less readily determined. Inserting filters that "blacken out" well-isolated resonances or stop the neutrons near the source with a shadow bar perturb the beam and do not measure the effects of collimator scattering or room return in the detector building. The "black" filter technique is most useful in the submillion-electron-volt region where the theoretical peak cross section of a resonance can be several orders of magnitude greater than the cross section from potential scattering. Therefore a reasonably thin sample will blacken out a resonance without perturbing the beam significantly at other

energies. But at higher energies, particularly in the million-electron-volt region, the peak-to-valley ratio decreases to first order as 1/E, and a rather thick sample is required to blacken out a resonance, which causes considerable distortion in the flux at other energies.

The neutron source can also give rise to an apparent time-independent background if the decay time of the sources of this background is considerably longer than the time between neutron bursts. This is particularly true at high repetition rates such as were used in these measurements.

To investigate the magnitude of the accelerator-related background, a 60-cm-long brass rod was inserted at the sample position and spectra were taken both with the detector in the neutron beam and outside the neutron beam. Also a spectrum was taken with the brass rod removed and the detector placed outside the neutron beam. All three spectra were flat except for two small broad peaks that occurred between the neutron bias energy (0.8 MeV) and about 3 MeV. The magnitude of these peaks was less than 4% of the constant background. We also found that the constant background observed in the open-beam spectrum below the neutron bias and on either side of the gamma-ray peak was greater than that accounted for by the background observed with the accelerator off, and that it decreased with increasing sample thickness. Apparently we have a time "independent" source of background from the target that has a decay time much longer than 3.2 μs but shorter than seconds since this background was completely absent just after shutting off the accelerator. We therefore corrected the data by subtracting from each channel a constant value that was determined by the average number of counts on either side of the gamma-ray peak and an accelerator-dependent value that was determined by the structure in the spectrum taken with the brass rod inserted in the neutron beam. The magnitude of the background correction varied from 3% of the open-beam spectrum at 1.5 MeV, 0.5% at 4 MeV, to 1% at 14 MeV.

As a check on our background correction, the peak cross section of the broad resonance at 3.5 MeV in carbon was measured with two different sample thicknesses. The samples had transmissions at the peak of 0.05 and 0.3. The peak cross sections obtained agreed to better than 1%, well within the statistical uncertainty on the data points in the peak region.

As a further check, a thick sample of ^{10}B (n = 0.9011 at/b) was run and the data compared with the thin sample data (n = 0.4509 at/b). The data were energy averaged into fairly wide bins that varied from 50 keV at 1 MeV to 200 keV at 15 MeV. The agreement over this energy region was better than ±0.5%.

D. In-Scattering Correction

The tight geometry of our TOF system ensures that the in-scattering correction will be small. Using the formula given by Bratenahl, et al.[8] we compute an overall in-scattering correction of approximately 5×10^{-5}, which is negligible and was thus ignored.

E. Summary of the Systematic Errors

From the previous discussions we estimate the systematic uncertainty in the transmission to be ±1.7%. This error is determined from the following estimates of the various sources of errors: sample thickness ±0.7%, background ±1%, normalization ±1%, and deadtime ±0.5%. Since the fractional uncertainty in the cross section is equal to the fractional uncertainty in the transmission multiplied by $1/n\sigma$ (where σ is the cross section), the systematic uncertainty in the cross section will be larger because, for our samples, $n\sigma$ is generally less than 1.

F. Accuracy of the Neutron Energy Scale

The accuracy of the neutron energy scale depends on the error in the flight path measurement, the stability of the electronics, the linearity of the time digitizer, the error in defining the centroid of the "gamma-flash" peak, and the difference in the effective thickness of the scintillator for low-energy neutrons as compared with that for high-energy neutrons or gamma rays.

The flight path was measured with a LASL-built Invar* steel tape system with digital readout. It had

*Carpenter Technology Corp., 150 West Bern St., Reading PA 19603

a reading accuracy of ±25.4 μm. The distance was measured in 15.24-m increments. The tape was supported by an aluminum platform that was positioned along the axis of the beam tube. Two independent measurements were made with the average of the two readings giving a distance to the front surface of the detector of 38.9145 ± 0.0015 m.

The electronic stability was measured by observing the drift in the centroid of the gamma-ray peak during a measurement. This drift was random with a maximum shift of less than one-quarter of a channel or 125 ps.

The integral linearity of the time digitizer is quoted by the manufacturer to be 0.005%. For a time span of 3.2 μs this would be equivalent to a maximum uncertainty in the last channel of 160 ps.

We estimate the uncertainty in defining the centroid of the gamma-ray peak to be about one-fifth of a channel or 100 ps.

The average distance a gamma ray travels in a scintillator before it creates a light pulse is one-half the thickness of the scintillator. This is also approximately true for very high energy neutrons. However, for low-energy neutrons more interactions take place near the incident surface than at the back surface. Thus the flight path for neutrons is different than that for gamma rays, which are used to define the zero flight time. This difference amounts to less than 1.2 mm or 87 ps for 1-MeV neutrons for the NE-110 detector and is somewhat less for the Pilot-U detector. Since this timing uncertainty becomes smaller with increasing neutron energy and is less than our resolution, the neutron energy scale was not corrected for this effect.

If we assume that all the errors contribute in quadrature, then the total uncertainty in the neutron energy scale in kiloelectron volts is $\pm 0.060E\sqrt{1.79E + 0.75}$ with E given in millions of electron volts.

IV. RESULTS

The total cross sections of ^{9}Be, ^{10,11}B, and ^{12,13}C from 1.0 to 9 MeV are presented in Figs. 3-12. Because of a shift in the neutron bias during the ^{12}C measurements only the data above 1.2 MeV are shown. The data from 1.0 to 1.5 MeV have been averaged over five channels. The boron and carbon data have been corrected for the minor isotopic impurities in the samples. The statistical uncertainties in the cross sections vary from a few per cent at 1.5 MeV to about 0.5% at 9 MeV for a 0.5-ns channel width.

The data from 4.0 to 13.5 MeV are presented in Figs. 13-17. These data have been averaged over five channels. The statistical uncertainty on each point in this region is less than a few tenths of a per cent. The data have been plotted with the vertical scale expanded (suppressing the origin) and the horizontal scale compressed to illustrate the large number of small resonances that are present in the data. If the data had been plotted on the scale of the previous figures, these resonances would not be readily discernible. For instance, the peak cross sections of the resonances between 6.5 and 7.5 MeV in ^{11}B (Fig. 15) are only a few per cent above the background cross section. Also, to extract this structure from the large background cross section requires high statistical accuracy in the data. Such data can be taken in a very short time using the beryllium source.

It is interesting to point out that the structure in ^{11}B from 6.5 to 7.5 MeV that corresponds to highly excited states in the residual nucleus ^{12}B has been observed recently by F. Ajzenberg-Selove, et al.[4] in the reaction ^{9}Be(^{7}Li,α)^{12}B. Their resolution was less than 40 keV and our resolution in this energy region is about 22 keV. The agreement between the two energy scales is excellent; for the narrow state at an excitation energy of 9585 ± 20 keV, we obtain an energy of 9583 ± 5 keV using 3.369 MeV for the recommended value[3] of the neutron binding energy in ^{12}B.

Because the total cross section of ^{12}C is often used as a standard, let us compare our results with the most recent evaluation of the cross section. For this purpose we used the ENDF/B-IV evaluation of the carbon cross section. Instead of comparing the two sets of cross sections by plotting them on the same graph, which would not have the sensitivity to show the small differences expected, we have made the comparison at selected energies and have presented the results in Table II. Our data have been averaged over the indicated energy intervals in order to improve the statistical accuracy on each data point and to smooth any minor fluctuations in the cross section in these intervals. Only statistical errors are given for these averages. The energy intervals were chosen to correspond to smoothly varying regions of

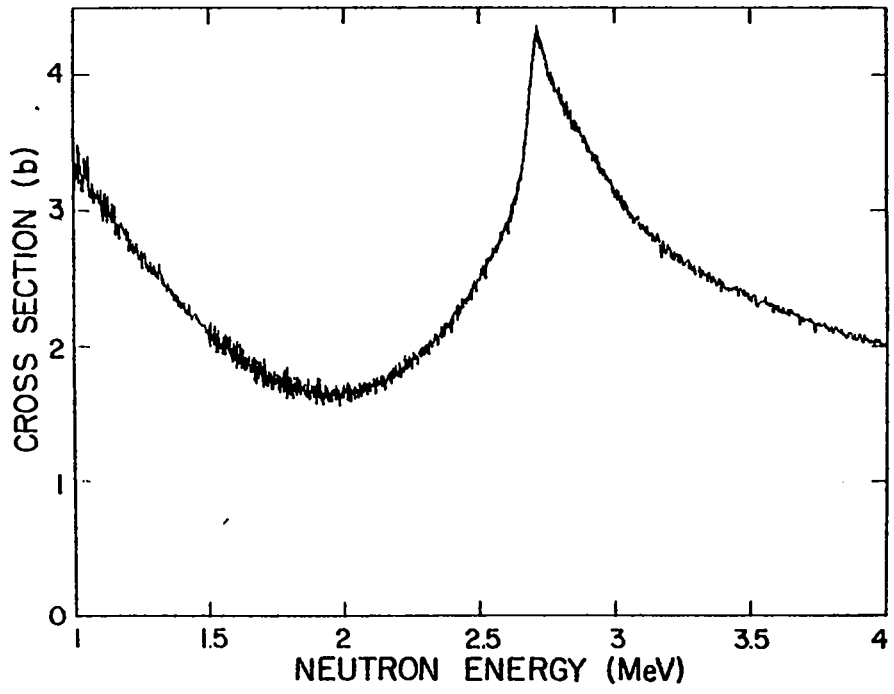

Fig. 3.
Total cross section of ^{9}Be from 1.0 to 4 MeV. The data below 1.5 MeV have been averaged over five channels.

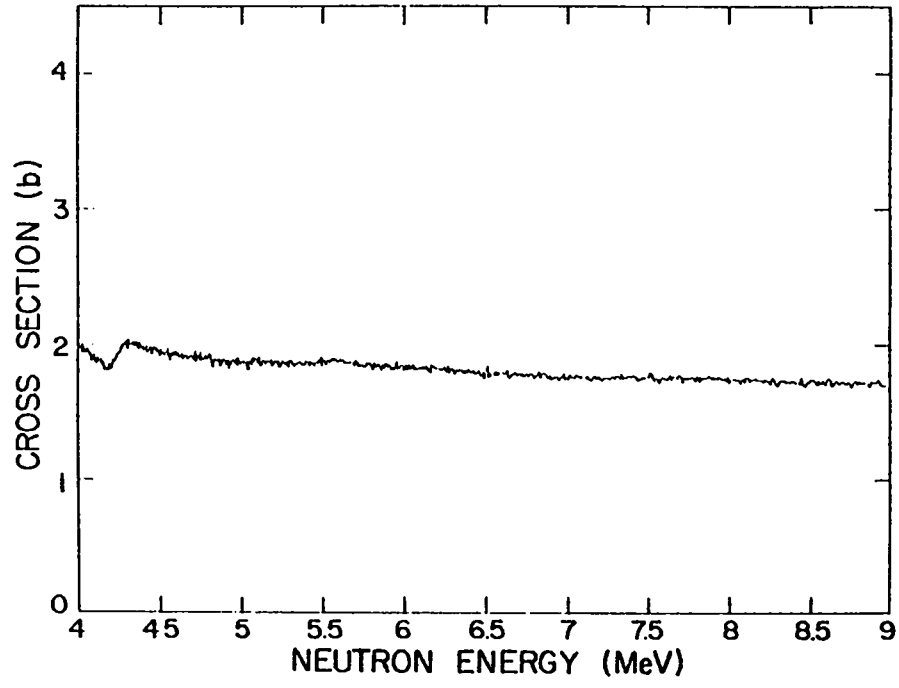

Fig. 4.
Total cross section of ^{9}Be from 4 to 9 MeV.

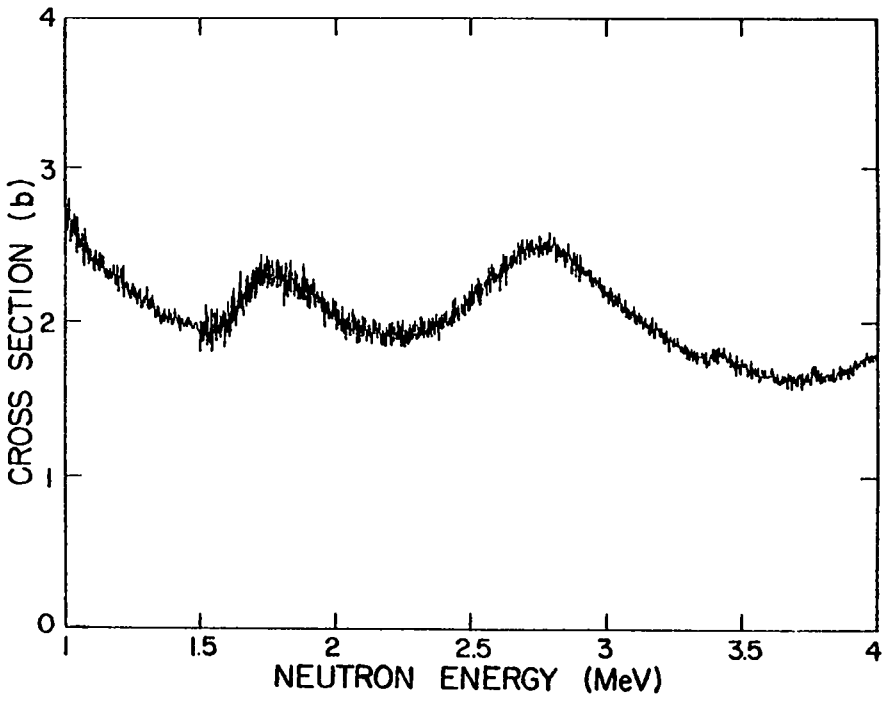

Fig. 5.
Total cross section of ^{10}B from 1.0 to 4 MeV. The data below 1.5 MeV have been averaged over five channels.

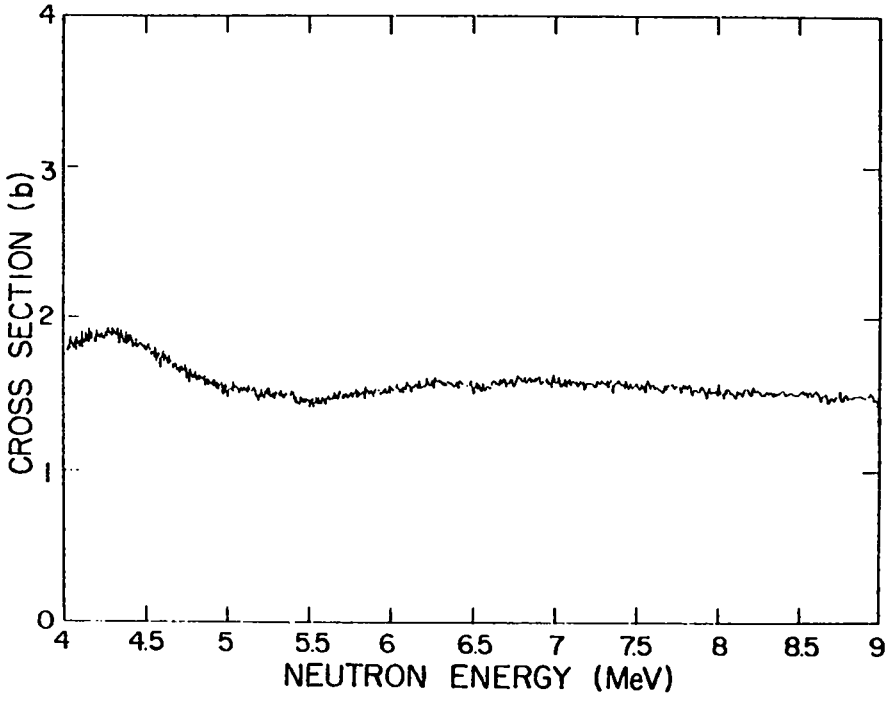

Fig. 6.
Total cross section of ^{10}B from 4 to 9 MeV.

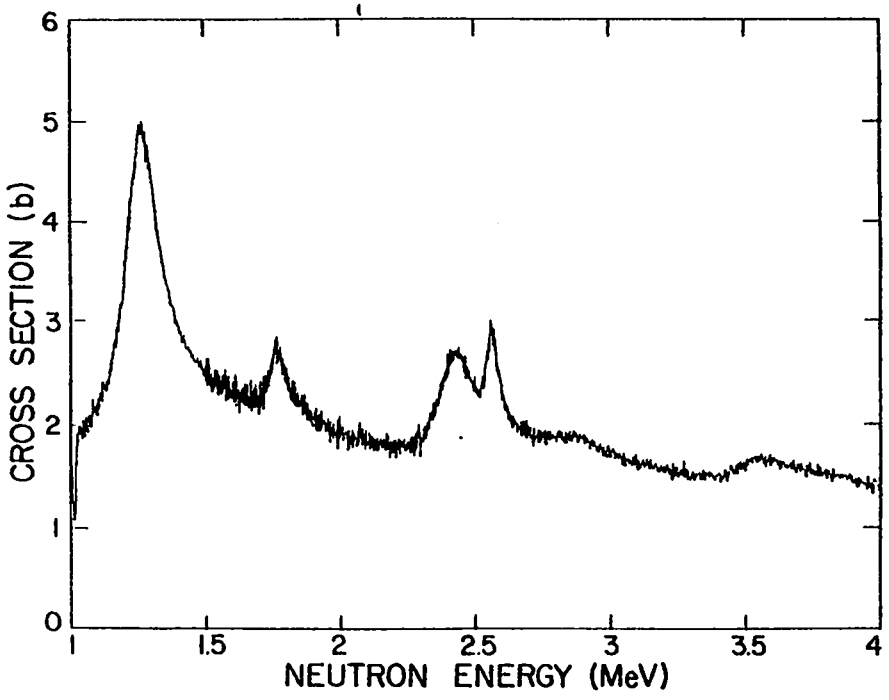

Fig. 7.
Total cross section of ^{11}B from 1.0 to 4 MeV. The data below 1.5 MeV have been averaged over five channels.

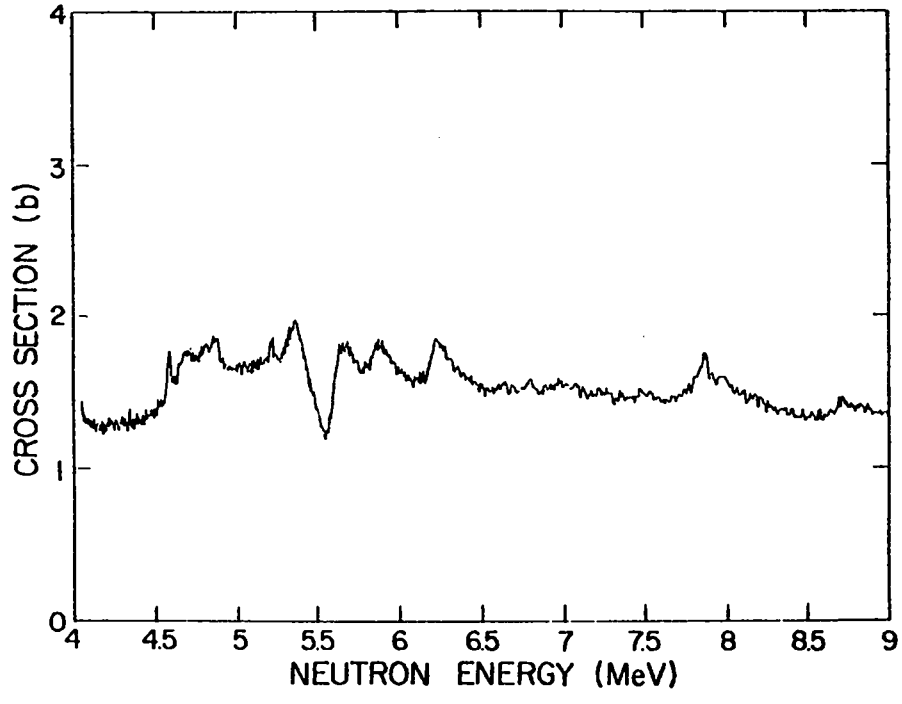

Fig. 8.
Total cross section of ^{11}B from 4 to 9 MeV.

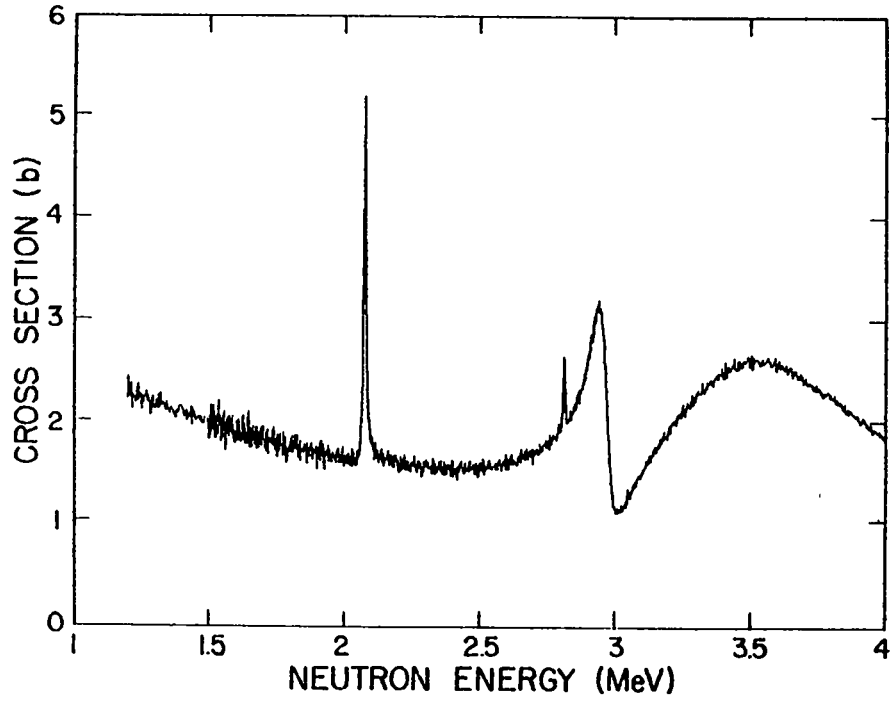

Fig. 9.
Total cross section of ^{13}C from 1.2 to 4 MeV. The data below 1.5 MeV have been averaged over five channels.

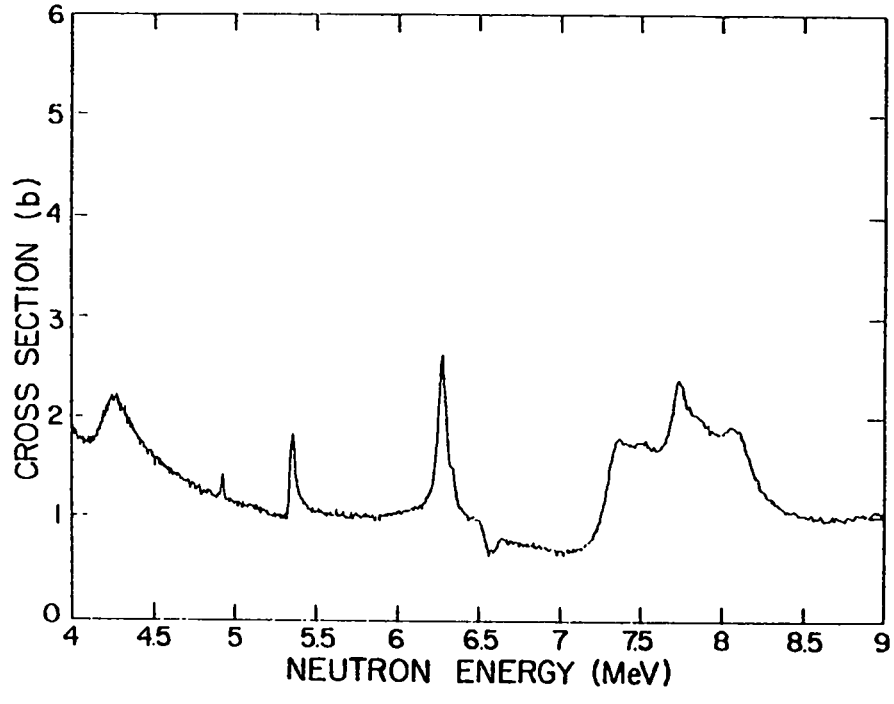

Fig. 10.
Total cross section of ^{13}C from 4 to 9 MeV.

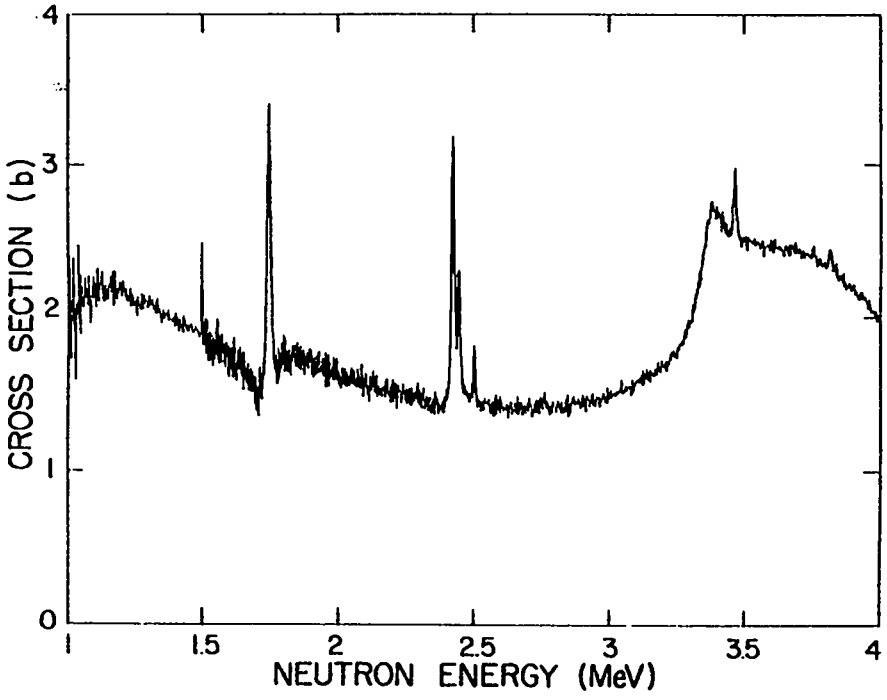

Fig. 11.
Total cross section of ^{18}C from 1.0 to 4 MeV. The data below 1.5 MeV have been averaged over five channels.

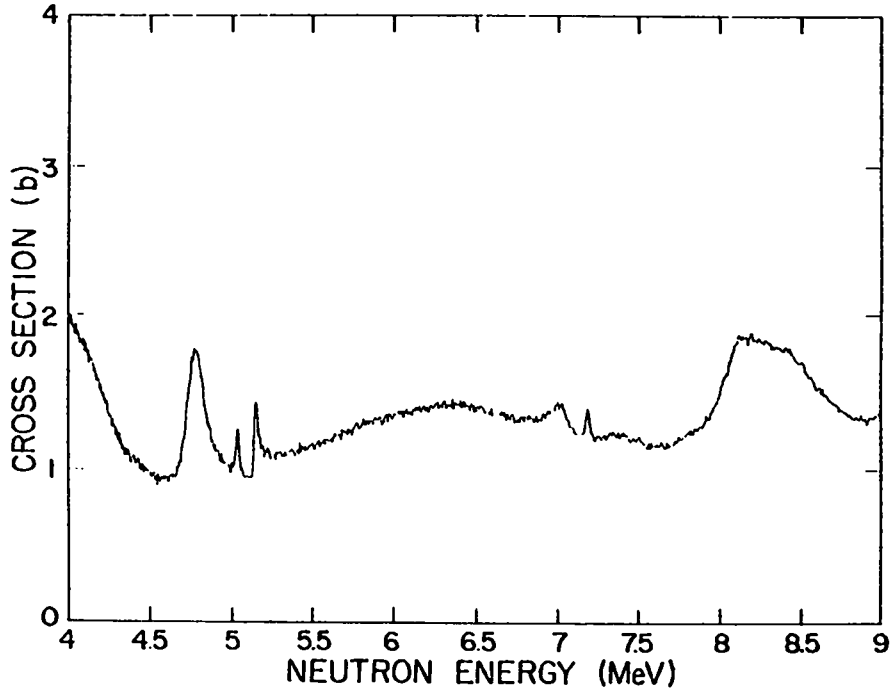

Fig. 12.
Total cross section of ^{18}C from 4 to 9 MeV.

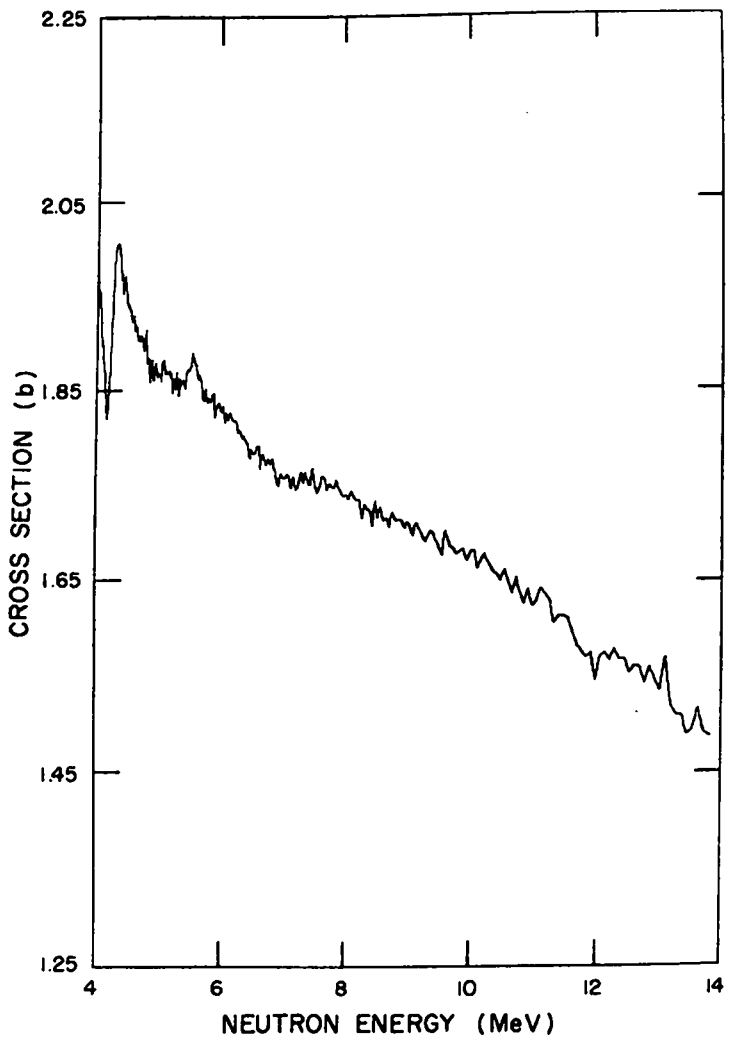

Fig. 13.
Total cross section of ^{9}Be from 4 to 13.9 MeV. Note the suppressed zero origin on the vertical scale. The data have been averaged over five channels.

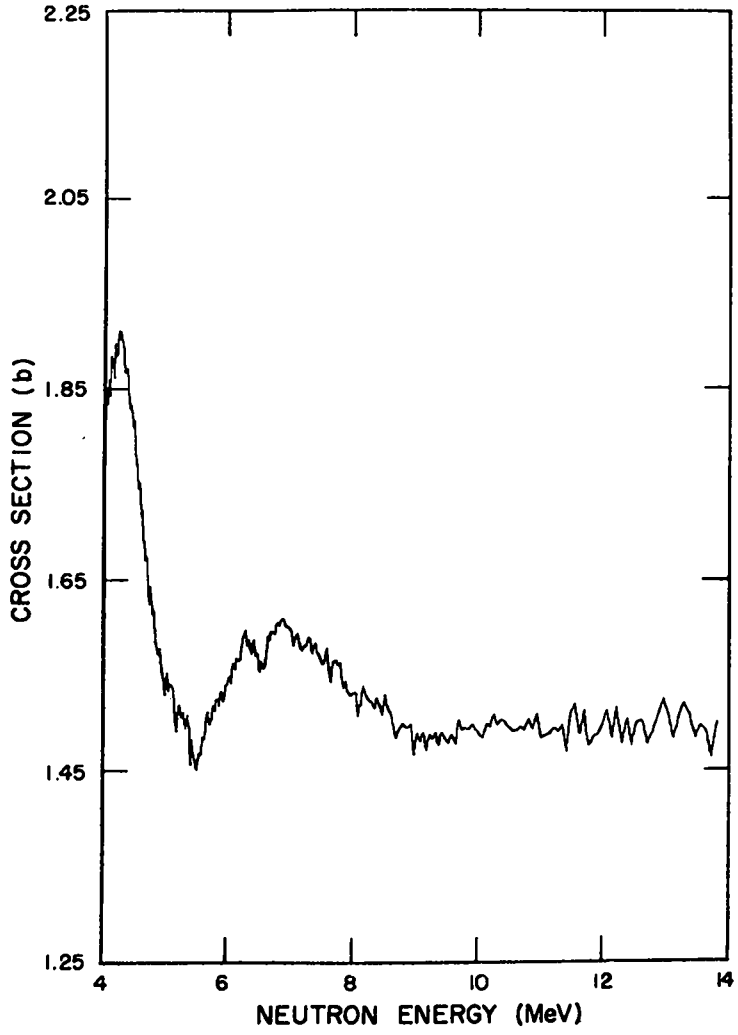

Fig. 14.
Total cross section of ^{10}B from 4 to 13.9 MeV. Note the suppressed zero origin on the vertical scale. The data have been averaged over five channels.

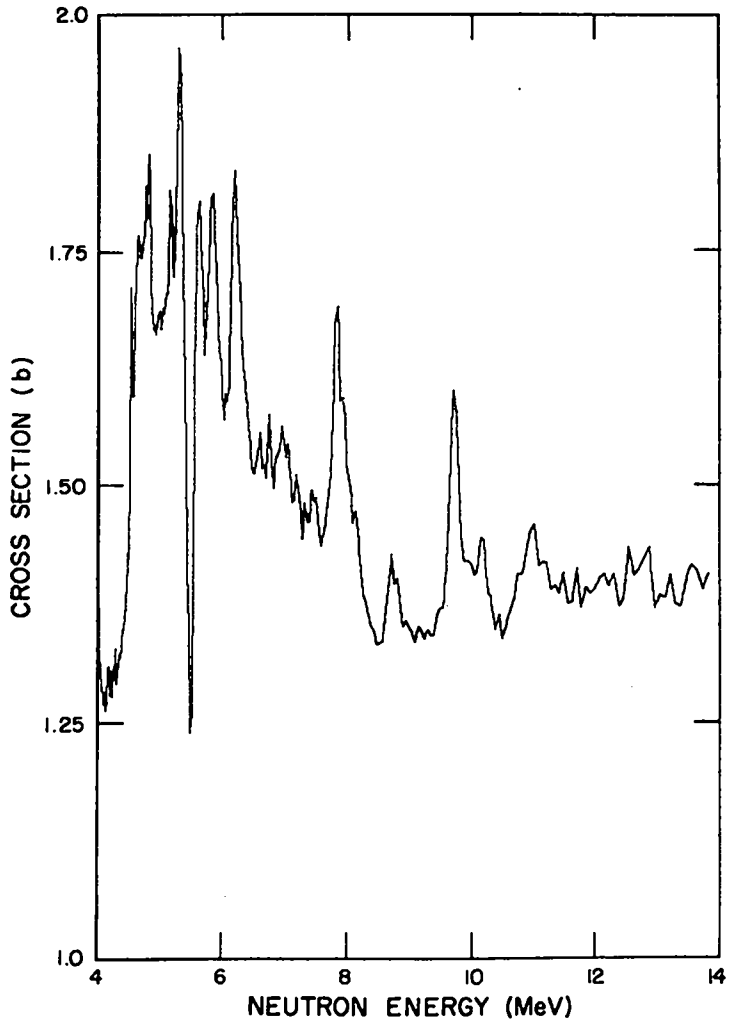

Fig. 15.
Total cross section of ^{11}B from 4 to 13.9 MeV. Note the suppressed zero origin on the vertical scale. The data have been averaged over five channels.

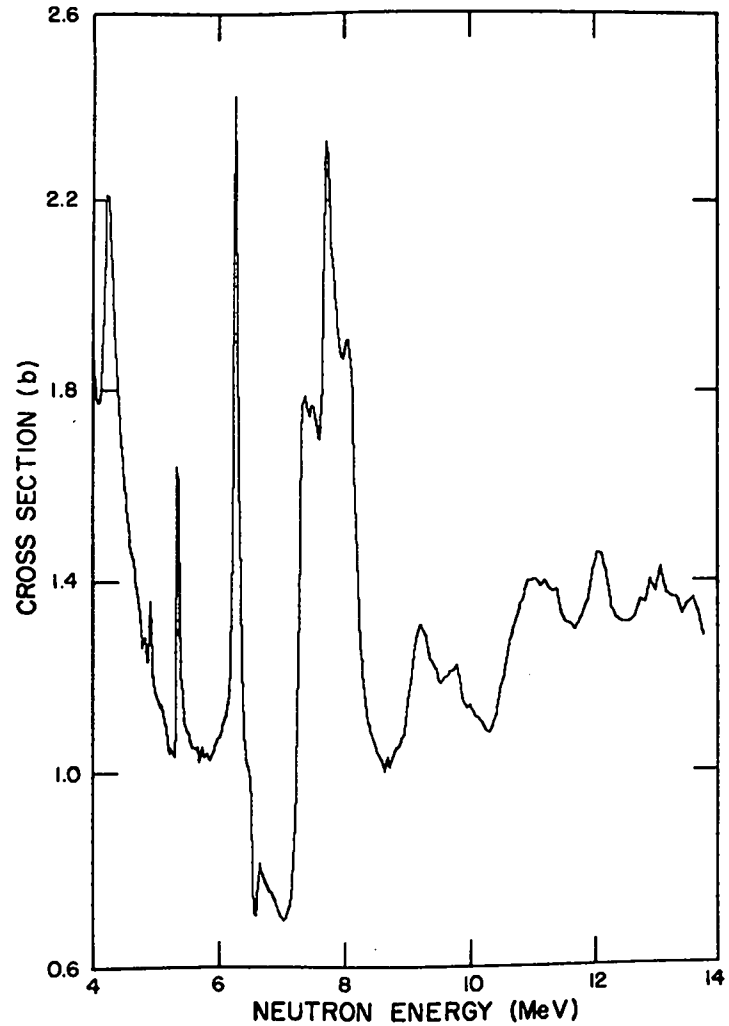

Fig. 16.
Total cross section of ^{12}C from 4 to 13.9 MeV. Note the suppressed zero origin on the vertical scale. The data have been averaged over five channels.

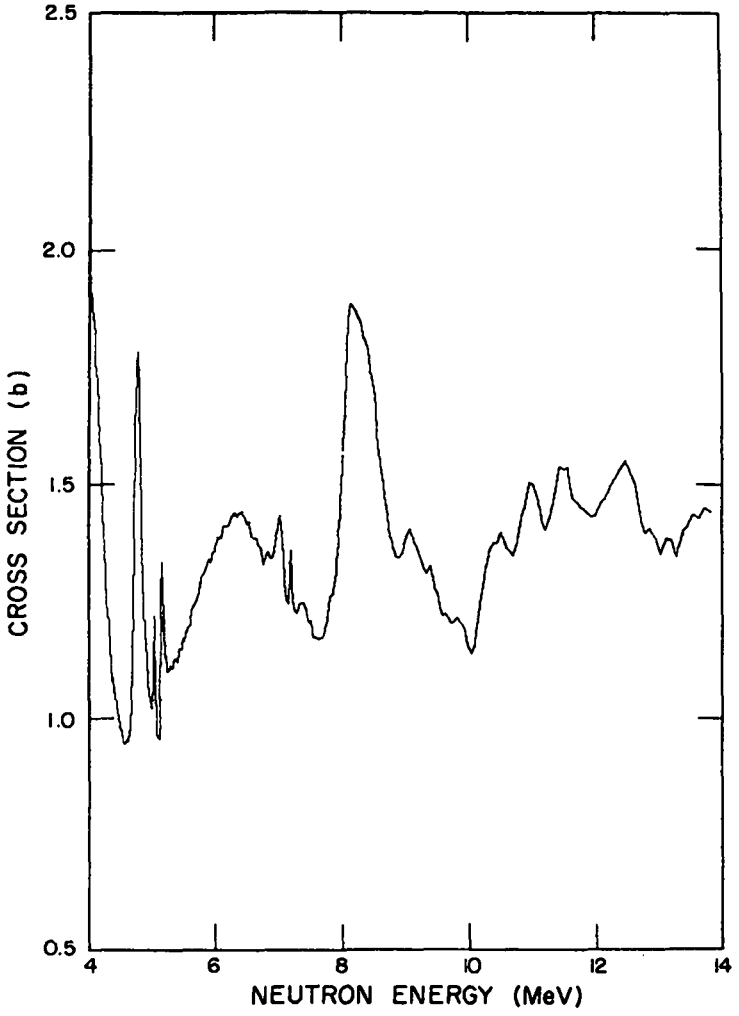

Fig. 17.
Total cross section of ^{13}C from 4 to 13.9 MeV. Note the suppressed zero origin on the vertical scale. The data have been averaged over five channels.

the cross section where more meaningful comparisons can be made. We have no explanation for why our values are systematically higher at the ends and lower in the middle of the energy region.

ACKNOWLEDGMENTS

We gratefully acknowledge the assistance of the members of the LASL Tandem Accelerator Group. We are indebted to A. N. Ellis for the mechanical design of the sample changer and to A. Greenwood for the electrical design of the sample changer interface. We would also like to thank M. G. Silbert and D. M. Drake for assistance in the data acquisition.

TABLE II

COMPARISON OF CARBON TOTAL CROSS-SECTION RESULTS (LASL) WITH THE ENDF/B-IV EVALUATION AT SELECTED ENERGIES

E_1 to E_2 (MeV)		LASL (b)	ENDF (b)	Difference (%)
1.495	1.505	2.089 ± 0.015	2.037	2.5
2.540	2.560	1.605 ± 0.006	1.589	1.0
3.580	3.620	2.611 ± 0.006	2.625	−0.5
4.990	5.010	1.181 ± 0.004	1.205	−2.0
6.985	7.020	0.700 ± 0.002	0.730	−4.2
8.600	8.700	1.027 ± 0.003	1.064	−3.5
10.20	10.30	1.094 ± 0.003	1.085	0.8
12.40	12.60	1.322 ± 0.004	1.310	0.9

REFERENCES

1. D. G. Foster, Jr. and D. W. Glasgow, "Neutron Total Cross Sections, 2.5-15 MeV. I. Experimental," Phys. Rev. **C3**, 576 (1971).

2. F. Ajzenberg-Selove, "Energy Levels of Light Nuclei A=11-12," Nucl. Phys. **A248**, 1 (1975).

3. A. Bratenahl, J. M. Peterson, and J. P. Stoering, "Neutron Total Cross Sections in the 7- to 14-MeV region," Phys. Rev. **110**, 927 (1958).

4. F. Ajzenberg-Selove, R. Middleton, and J. D. Garrett, "Energy Levels of ^{12}B," Phys. Rev. **C12**, 12 (1975).